RESEARCH ARTICLE

Analysis of rainfall infiltration and its influence on groundwater in rain gardens

Jiake Li[1] · Fan Li[1] · Huaien Li[1] · Chao Guo[1] · Wen Dong[1]

Abstract

The dynamic observation data on groundwater level and water quality were obtained from rain gardens #2 and #3 from May to October 2016. The water balance method and 2D numerical simulation of variable saturation zone were used to calculate rainfall infiltration recharge coefficient, water supply, and evaporative discharge of rain garden. These parameters were used to simulate and explore the impact of rainfall infiltration in rain gardens on groundwater level and water quality. The groundwater depth of rain gardens was mainly affected by the concentrated infiltration of rainfall. The variation range of groundwater depth was approximately 4.298 ± 0.031 mm for J1, 3.9364 ± 0.097 mm for J2, and 4.0958 ± 0.064 mm for J3, and the specific yield was 0.208. Groundwater quality was naturally attenuated and would not threaten the safety of groundwater at a certain scale. Visual MODFLOW was used to simulate groundwater flow and conduct parameter sensitivity analysis to determine the main influencing factors of garden groundwater level change. Results showed that rainfall recharge was crucial to module sensitivity.

Keywords Rain garden · Concentrate infiltration · Groundwater · Numerical simulation · Sensitive analysis

Introduction

Ecological problems caused by urban rainwater are incrementally aggravated by the acceleration of urbanization. These problems include urban storm floods, urban water logging, water pollution, shortage of water resources, increased risk of urban flooding, reduced capacity of urban drainage systems, lowered groundwater level, and loss of aquatic habitats (Yu et al., 2015). Developed western countries have implemented many measures to solve these issues, and such measures include best management practices (Zimmer et al. 2007) and low-impact development (LID) in the USA, water-sensitive urban design (WSUD) in Australia, sustainable urban drainage system in the UK (Scholz and Grabowiecki 2007), and low-impact urban design and development in New Zealand (Van 2007). China has proposed the idea of building a sponge city with Chinese characteristics and began

to study and analyze the water-logging problems in Chinese cities in 2014 (Wu et al. 2016).

The sponge itself has two characteristics of moisture and mechanics. The moisture characteristics refer to the properties of sponge water absorption, water retention, and water release. The mechanical characteristics refer to the rebound, compression, recovery, and other properties of the sponge itself. Sponge cities can be like a sponge that has good "flexibility" in adapting to environmental changes and coping with natural disasters. When it rains, they absorb, store, infiltrate, and purify water. Rain gardens are typical rainwater retention facilities in LID that use rainwater from recessed greenery to reduce stormwater runoff and pollution from the source and recharge groundwater, landscape water, or other urban rainwater. Many studies have been performed on the regulation and control of storm runoff in rain gardens, the reduction of peak flow, and the purification of rainwater quality (Yang et al. 2013; Li et al. 2010). These studies have helped improve and supplement groundwater and reduce storm runoff (Tang 2016).

Machusick et al. (2011) found that precipitation more than approximately 18 mm leads to large increases in groundwater elevation at an upgradient control well located near the edge of a large grass field. Watson et al. (2018) determined the importance of incorporating short-term recharge event modeling for improving recharge estimates through evaluating a west coast in South

---

✉ Jiake Li
  xaut_ljk@163.com

1 State Key Laboratory of Eco-Hydraulics in Northwest Arid Region of China, Xi'an University of Technology, Xi'an 710048, China

Africa. Jia et al. (2018) found that the infiltration of rainwater runoff can effectively replenish the groundwater when the groundwater level of the rain garden is below 2–3 m. Guo et al. (2017) identified that the concentrated infiltration of rainwater gardens is conducive to recharging groundwater, but the negative impact on groundwater quality is unobvious. Runoff from the surface of the urban rain garden is filtered through the unsaturated zone of the soil and then enters the groundwater. This process involves the complexity in intercepting moisture in the unsaturated zone of the soil. While many factors influence the base flow from aquifers, the most important variable is the rate of groundwater recharge. Various approaches can be used to estimate recharge, but essentially, they can be grouped into three methods, namely, (1) physical, such as water table fluctuation (WTF) (Crosbie et al. 2005) or channel water budget (Rantz 1982); (2) chemical, such as chloride mass balance (Ting et al. 1998) or applied tracers (Forrer et al. 1999); and (3) numerical, such as rainfall modeling (SWAT, Arnold et al. 2000) or variably saturated flow modeling (HYDRUS, Phillips 2006; Visual MODFLOW, Van 2007). For the physical, WTF is unsuitable for calculating rainfall recharge in the depression storage area. For the chemical, the method of specific yield reverse thrust and Visual MODFLOW are used because no relevant data are collected. However, the amount of pollutants entering the groundwater is possible to increase and exert a negative impact on the water quality. Therefore, studying whether rain gardens can regulate urban rainfall runoff and whether they will have adverse effects on the groundwater environment is an important scientific problem for the construction of rainwater gardens.

A fundamental understanding of groundwater analysis in rain gardens is needed because of the complexity and the importance of rain garden concentration infiltration. The objectives of this work are the following: (i) to determine the impact of concentrated rainwater infiltration on groundwater quality through collecting and analyzing groundwater samples before and after rainfall. The concentration change processes of phosphorus (P), chemical oxygen demand (COD), and nitrogen (N) in groundwater are to be quantitatively analyzed. (ii) To clarify the influence of rainwater infiltration on the groundwater table through measuring the groundwater depth before and after rainfall and studying the rainfall recharge and media permeability coefficients. (iii) To simulate the annual change of groundwater level caused by concentrated infiltration of rain garden by establishing a numerical model of groundwater suitable for small areas.

Materials and methodology

Hydrology and climate

The rain gardens in this study are located on the campus of the Xi'an University of Technology in Xi'an, Shaanxi Province, China. The city of Xi'an is in Northwest China (107° 40′–109° 49′ E and 33° 39′–34°45′ N), which has a temperate continental climate. The soil layer is thick and homogeneous in this area, thus providing good groundwater occurrence. The average annual temperature is 13.3 °C, the annual average atmospheric precipitation is 580.2 mm, and the average annual evaporation is 990 mm. The geographical location, annual rainfall, and drought and flood conditions are shown in Fig. 1.

Monitoring system overview

The monitoring task involved rain gardens #2 and #3 (Fig. 2a, c). The structures of #2 and #3 are shown in Fig. 2b, d. Rain garden #2, which was used for collecting roof rainwater, has a depth of 20 cm and an area of approximately 30.24 m^2. The confluence ratio is 20:1, the runoff coefficient is 0.9, the confluence area is 604.7 m^2, and the structure is planted soil. A 45° triangular weir was placed at the inlet of the rain garden, and a 30° triangular weir was provided at the overflow to calculate confluence. Rain garden #2 was planted with black-eyed Susan, marigold, Changchun, and other plants.

Rain garden #3 was built in 2012. The flapper in the middle was used to divide #3 into two subsections (Fig. 2d). One part is waterproof, with a perforated tube mounted on the V-notch weirs of 30° at the bottom, whereas the other part is permeable without outflow. Inflows of the two pars were measured with pressure transducers mounted on V-notch weirs of 30° installed at the inlet. They have the same plants as #2. Each of the subsections is oval and is 6.2 m and 2 m in diameters. The aquifer has a thickness of 50 cm, and it receives rainwater from roofing and pavements. The confluence ratio is 15:1, the runoff coefficient is 0.9, the garden area is 9.74 m^2, and the convergence area is 155.84 m^2. The structures of rain gardens are shown in Table 1. The hydrogeological profile of the study area is shown in Fig. 3.

The water sample was collected and monitored for J1 and J3 in May 2016 to analyze the influence of centralized infiltration of rain gardens on the groundwater quality and groundwater depth. Water sampling and groundwater depth monitoring for J2 were conducted in July 2016 (Fig. 4). J1 is the control well and approximately 40 m away from rain gardens #2 and #3. J1 is not affected by the outside world. The three groundwater wells possess a depth of approximately 4.0 m and are mainly used to monitor changes in groundwater depth and groundwater quality (COD, N, and P).

Hydrogeological condition

This work reviewed the influence of the concentration infiltration of rain gardens on the groundwater regime and groundwater quality. The fixed head-to-water boundary was proposed to determine the recharge and discharge of the study

Fig. 1 Location of the study area
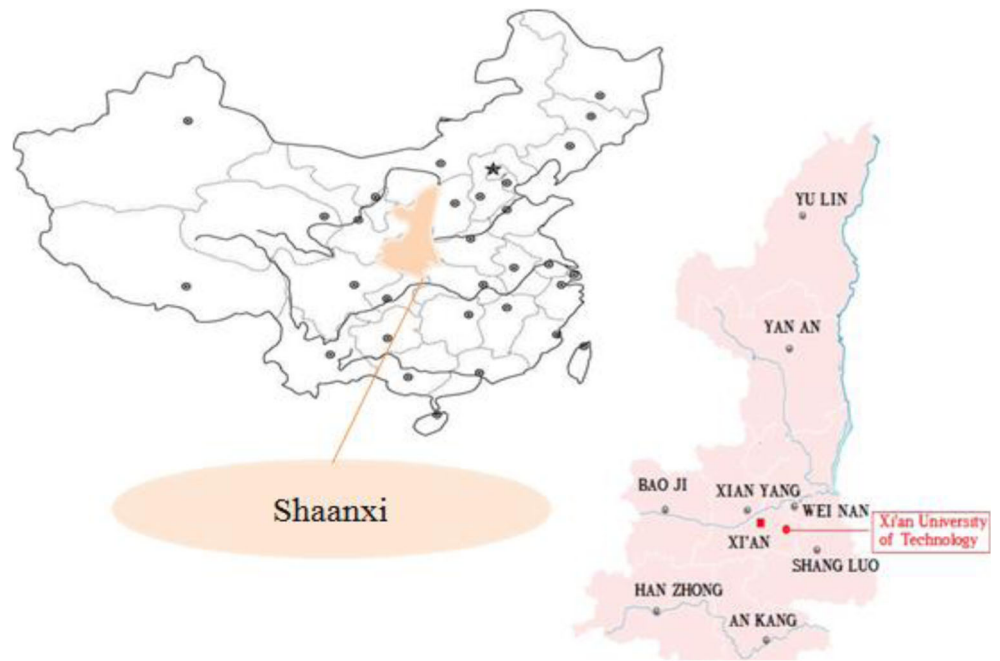
area due to the small infiltration range and different precipitation infiltration rates. The determination of the fixed boundary head was based on the long-term simultaneous measurement of groundwater level data of J1. The recharge of the simulated area included rainfall and water flow movement in the surrounding area in case of the original bare land. The
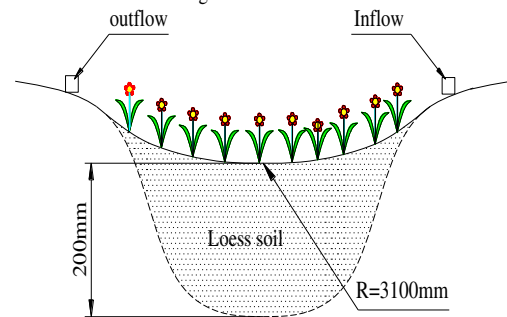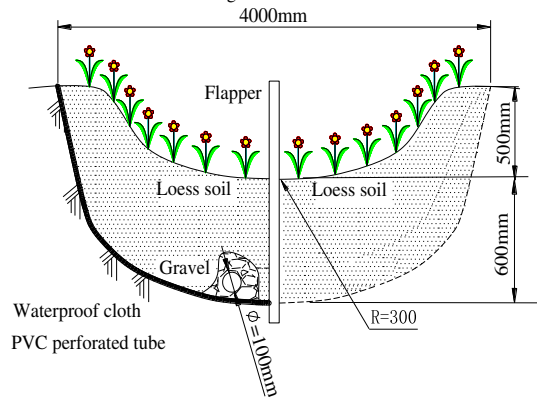

Fig. 2 Two rain gardens in the study area

Table 1 Rain garden structure

Rain gardens		Size	Area	Confluence area	Bottom treatment	Filters and thickness		Confluence area ratio	Underlying surface
#2		Long axis × minor axis × depth = 7 m × 5.5 m × 0.35 m	30.24 m²	604.7 m²	Permeable	Aquifer layer	20 cm	20:1	Roof
						Loess soil	20 cm		
#3	A	Long axis × minor axis × depth = 6 m × 2 m × 1.1 m	4.87 m²	77.92 m²	Waterproof	Aquifer layer	50 cm	15:1	Roof and concrete pavement
						Loess soil	45 cm		
						Gravel	15 cm		
	B	Long axis × minor axis × depth = 6 m × 2 m × 1.1 m	4.87 m²	77.92 m²	Permeable	Aquifer layer	50 cm		
						Loess soil	60 cm		

consumption included evaporation and supply to the surrounding area. The groundwater in the simulated and surrounding areas had no exchange of water flow and was finally determined to be the fixed head boundary in the absence of man-made mining. The velocity head of the study area was insignificantly different. Therefore, the position head was used as the total head, with a boundary head of 16 m.

Monitoring method

A total of 55 sets of groundwater level data for 12 rainfall events were collected in 5 months (May to October 2016). An instrumentation device capable of detecting the rainwater runoff process was installed at the inflow port of the rain garden to detect each rainfall process. A triangular raft was installed in the inflow and overflow of each rain garden in the study area, and the groundwater depth was monitored in real time by a pressure sensor and a paperless recorder, thereby obtaining a real-time flow process. Water samples were taken at the inflow, overflow, and drain at regular intervals, followed by chemical analysis.

Climate and rainfall

The monitoring indexes mainly included temperature, relative humidity, and rainfall on the day of sampling. The rainfall data

were obtained at meteorological station. The meteorological station is on the roof of the building of Institute of Water Resources, Xi'an University of Technology, Xi'an, Shaanxi (Fig. 4).

Groundwater levels

Groundwater depth was measured once before each rainfall event and on the first, third, fifth, and seventh days after rainfall in the rain gardens. If the two rainfall intervals are long, the monitoring frequency can be increased to observe the continuous impact of the rainfall on the groundwater level. The monitoring frequency was higher in the wet season than in the dry season because the groundwater level changes frequently in the wet season. This condition could improve the consistency between the experimental monitoring and the actual situation. The groundwater depth was measured by a float ball (Fig.5). The influence of rain garden concentration infiltration on groundwater was compared between monitoring wells (J2, J3) and control well (J1). And t test was used in statistical analysis to compare the significance of the difference between the observation results of J2, J3, and J1. The confidence level of difference significance was relatively strict, 0.01, because the groundwater level had certain fluctuation.

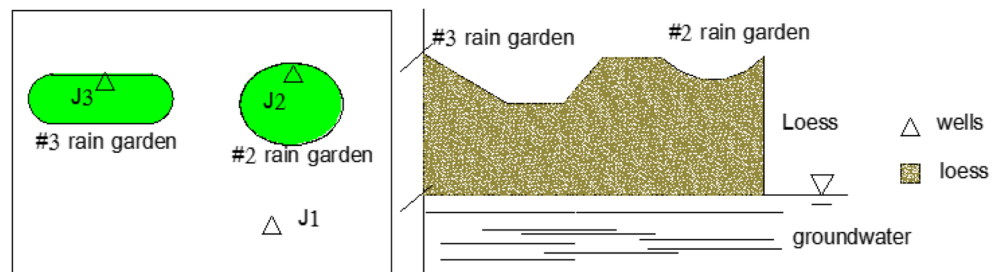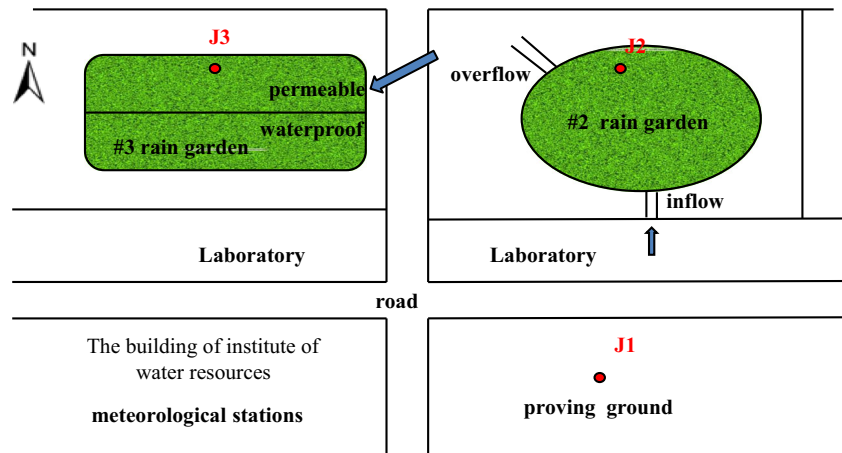**Fig. 3** Hydrogeological profile of the study area

Fig. 4 Underground wells and meteorological station location

Groundwater quality

The groundwater samples were stored in a refrigerator at −4 °C, and analysis was completed within 3 days. NH_4^+-N was measured by continuous flowing analysis (SKALAR, Holland). TP was measured by an ultraviolet spectrophotometer (DR5000). SigmaPlot 12.5 (developed by Systat Software Company, USA; the supplier is Beijing ND Times Technology Co., Ltd. Beijing, China) and SPSS 20.0 (developed by Stanford University, California, USA) were used for data analysis. t test was used in statistical analysis to compare the significance of the difference between the observation results of J2, J3, and J1. The confidence level of difference significance was relatively strict, 0.01, because the groundwater quality presented certain fluctuation.

Recharge

The Reynolds number of groundwater flow in natural interstitial aquifers is much smaller than the critical Reynolds number and the critical number for hydraulic slopes. Therefore, most of the natural groundwater in the laminar state is influenced by Darcy's law. Unsaturated soil moisture generally performs 1D vertical movement to accept the atmospheric vertical recharge. The infiltration coefficient of


Fig. 5 Underground water sample collector

precipitation and specific yield are important hydrological parameters in groundwater-related research. Precipitation infiltration recharge and surface water infiltration recharge are important elements of groundwater resource formation. The quantity of groundwater reserves is closely related to precipitation infiltration rate. Precipitation infiltration rate is highly important in appropriately evaluating the transformation of three types of water, namely, surface water, soil water, and groundwater. Groundwater recharge types (Lu et al. 2015) include direct recharge, localized recharge, and indirect recharge (Fig. 6a). The source of groundwater runoff of rain garden mainly includes direct recharge and localized recharge (Fig. 6b). The losses of groundwater replenishment by rainfall mainly include interception by vegetation, evaporation, absorption by soil, depression storage, and runoff. Loheide et al. (2005) used the variable saturated zone 2D numerical simulation (VS2D) to propose a reasonable formula for the instantaneous water supply of different media when the depth of burial is shallow (Eq. 1). The value of saturated water content of the soil is between 40.2 and 50.0% in the Loess Region, and the value of surface water content before rain is between 19.5 and 29.1% in rain gardens. The value of gravity-specific yield is between 0.111 and 0.305, and the average is 0.208 as the initial value. Gerla (1992) proposed a method for calculating gravity-specific yield that is suitable for shallow groundwater levels and used this method to calculate the amount of rainfall infiltration recharge (Eq. 2). Schilling calculated the groundwater evapotranspiration in the barnyard grass growing area in the Walnut Creak Wetland in Iowa, USA, as shown by Eq. 3 (Schilling and Kiniry 2007). The interception by vegetation, height difference of groundwater depth, gravity-specific yield, groundwater recharge, and evaporation of rain gardens #2 and #3 relative to the rainfall infiltration coefficient were calculated according to the following formulas, as also shown in Table 2:

$$S_y = \theta_s - \theta_{surface}, \tag{1}$$

Fig. 6 Recharge mechanism. **a** Groundwater recharge mechanism. **b** Rain garden recharge mechanism

Note : The thicker the arrow, the greater the flow
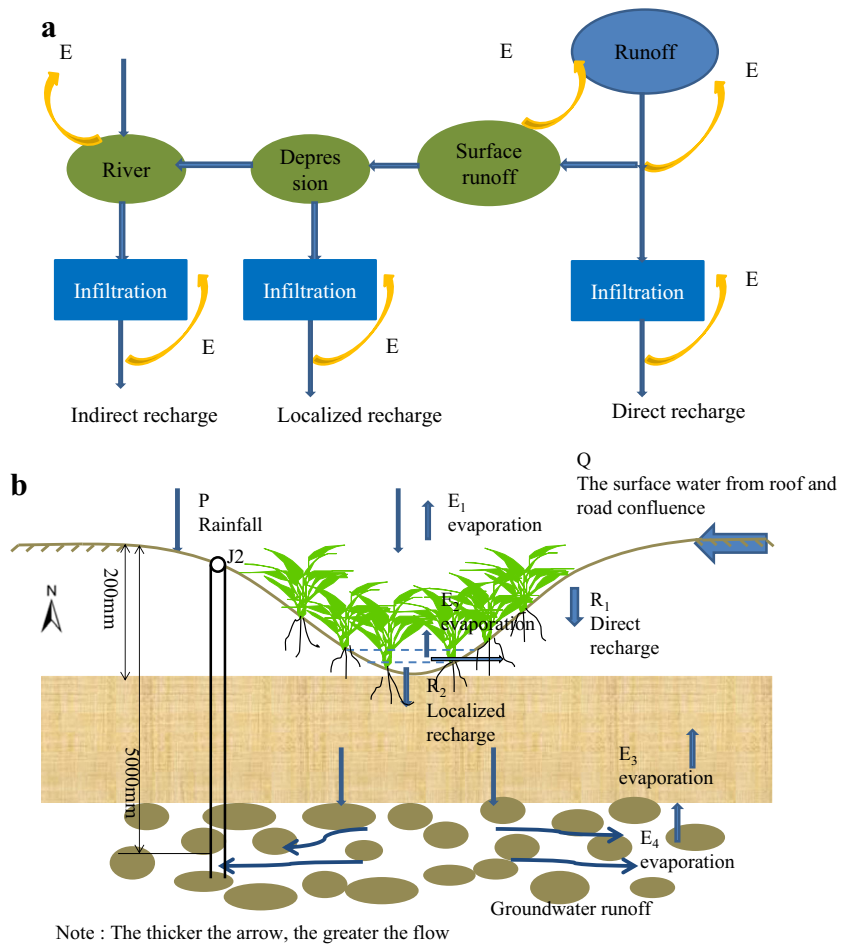
$$S_y = \frac{P_r}{\Delta H}, \tag{2}$$

$$E_{Tg} = \sum (d_i - d_{i-1}) * S_y, \tag{3}$$

where S_y is the gravity-specific yield, θ_s is the water content of saturated soil (%), $\theta_{surface}$ is the surface water content before rain (%), P_r is the precipitation recharge (mm), $\triangle H$ is the height difference of groundwater depth (mm), d_i is the water depth on day i (mm), d_{i-1} is the water depth on day $i+1$ (mm), and E_{Tg} is the evaporation coefficient of precipitation (mm).

Table 2 Statistical results of groundwater depth in the monitoring wells

Well number	Monitoring period			Within 3 days		
	Avg ± SD	t	p	Avg ± SD	t	p
J1	4.2984 ± 0.031			4.2978 ± 0.032		
J2	3.9364 ± 0.097	0.777	0*	3.9322 ± 0.103	0.765	0*
J3	4.0958 ± 0.064	0.743	0*	4.0911 ± 0.062	0.751	0*

*$p < 0.01$, the difference is significant

Groundwater models and method

Visual MODFLOW

Visual MODFLOW is a computer program developed by the United States Geological Survey (Raj and Prabhakar 2016). Visual MODFLOW is a comprehensive software developed by Canada's Waterloo Hydrogeology Company. The software is based on MODFLOW, MODPATH, MT3D, RT3D, and Win PEST models. Visual MODFLOW is internationally popular professional software for 3D visualization of groundwater resource evaluation and prediction. This software is convenient and effective for simulating water flow, solute transport, and migration response. Visual MODFLOW uses the finite difference method, which has powerful visualization, simple solution method, wide application, excellent numerical simulation capability, and simple 3D modeling (Van 2007).

Flow equation

MODFLOW, a widely used groundwater flow model, employs a 3D finite difference method. A 3D transient flow

model comprises the basic equation of normal density groundwater, as shown as follows:

$$\frac{\partial}{\partial \chi}\left(\kappa_\chi \frac{\partial h}{\partial y}\right) + \frac{\partial}{\partial y}\left(\kappa_y \frac{\partial h}{\partial y}\right) + \frac{\partial}{\partial z}\left(\kappa_z \frac{\partial h}{\partial z}\right) - q = \mu_s \frac{\partial H}{\partial t} \quad (4)$$

The definite conditions are as follows:

$$H|_{B1} = H(x, y, t), \quad (5)$$

$$H\frac{\partial H}{\partial n}\bigg|_{B2} = q(x, y, t), \quad (6)$$

where K is the permeability coefficient of the subterranean aquifer medium along the x, y, and z dimensions (L/T); h is the phreatic depth; μ_s is the specific yield; H is the water level; and q is the source and sink of groundwater. Equation 5 is the boundary of fixed head; B_1 is the first boundary; Eq. 6 is the boundary of fixed flow; B_2 is the second boundary; and n is the normal direction outside the boundary.

Solution selection

MODFLOW can be divided into a strongly implicit procedure (SIP), successive over-relaxation, and preconditional conjugate gradient method. SIP requires no data experiment and has a high convergence rate when selecting parameters. Therefore, this simulation used MODFLOW's default SIP and adopted the default parameter combination for numerical calculation (Fan et al. 2015).

Sensitivity

Morris screening includes one variable at a time. The parameter value and the operating model for model output values are randomly changed within the scope of the threshold value of the variable to calculate the model output and to input the rate of change of the model parameters to represent the influence of parameter change on the model. On the basis of the Morris screening method, a parameter is taken as a variable x_i, and the remaining parameters are kept fixed. The variable x_i is randomly changed within the value range of the variable. The result of the objective function $y(x_i)$ that corresponds to different x_i values is obtained by operating the model. The influence value e_i is used to indicate the influence degree of the parameter variation on the model simulation result, as shown as follows:

$$e_i = (y - y_0)/\Delta_i, \quad (7)$$

where e_i is the Morris coefficient, y is the model output after the parameter changes, y_0 is the model output before the parameter changes, and Δ_i is the amplitude of parameter i.

The modified Morris screening method allows independent variables to be varied by a fixed percentage of the step size,

and the final sensitivity discriminant factor is the average of multiple Morris coefficients, as shown as follows:

$$S = \sum_{i=1}^{n} \frac{(Y_{i+1} - Y_i)/Y_0}{(P_{i+1} - P_i)/100}/n, \quad (8)$$

where S is the factor of parameter sensitivity, Y_i is the output value of the ith run of the model, $Y_i + 1$ is the output value of the $(i + 1)$th run, Y_0 is the initial value of the calculated result after parameter adjustment, P_i is the percent change of the parameter value after the ith run model relative to the initial parameter value, $P_i + 1$ is the percent change of the parameter value after the $(i + 1)$th run model relative to the initial parameter value, and n is the running time of the model. According to the S value of the parameter, Morris screening divides the sensitivity of parameters into four categories, namely, $|S| \geq 1$ is the highly sensitive parameter, $0.2 \leq |S| < 1$ is the sensitive parameter, $0.05 \leq |S| < 0.2$ is the moderately sensitive parameter, and $0 \leq |S| < 0.05$ is the insensitive parameter.

Monitoring and analysis

Influence of concentrated infiltration on groundwater level

A total of 55 sets of groundwater level data for 12 rainfall events were collected in 5 months (May to October 2016). The relationship between a dynamic change in groundwater depth and rainfall is shown in Fig. 7a. The data of groundwater in 2013 and 2014 are also given in Fig. 7b (Tang 2016). The groundwater table changed with rainfall in the study area, and the groundwater depths of J2 and J3 were smaller than that of J1 during the entire dynamic change monitoring, that is, the concentrated infiltration decreased the groundwater depth. The groundwater depth of J1 remained stable, the trends of J2 and J3 were consistent, and the groundwater depth of J2 was higher than that of J3. During the rainy season, the rainfall area had abundant water, and the groundwater depth was "jagged." Groundwater depth showed rapid rise and fall characteristics at the beginning and end of a rainfall event, thereby reflecting the response of groundwater level to rainfall. The variation range and statistical results of the groundwater depth observations of #2 and #3 were listed within the entire monitoring period and within 3 days after rainfall (Table 2). The average depth of groundwater for monitoring wells J2 and J3 was significantly smaller than that for control point J1 during the monitoring period, the average depth of groundwater for both monitoring wells within 3 days after rainfall was also significantly smaller than the control well, and the groundwater levels of J2 and J3 were raised by an average of 0.3 m. The standard deviation was small, which indicated that the groundwater level at the infiltration recharge point was high and the water level was stable.
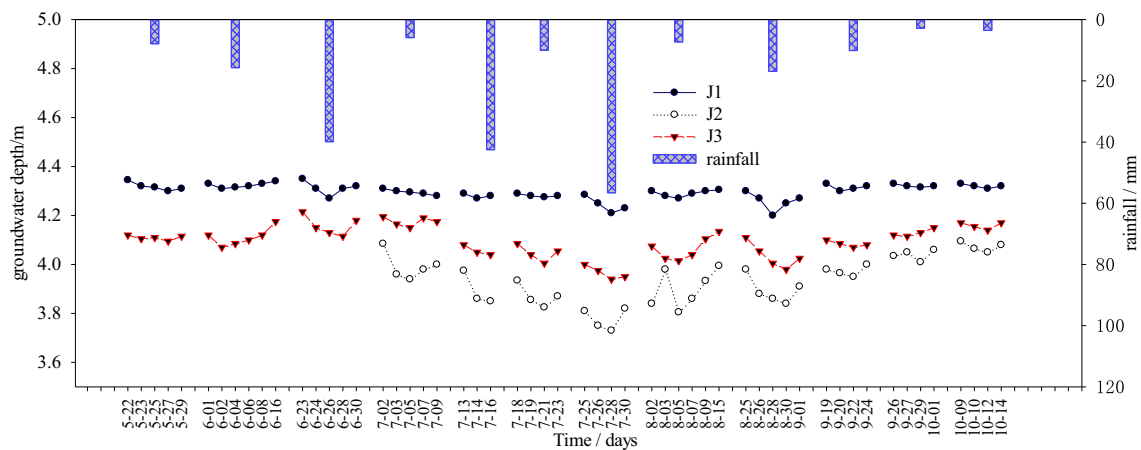
a Data of 2016
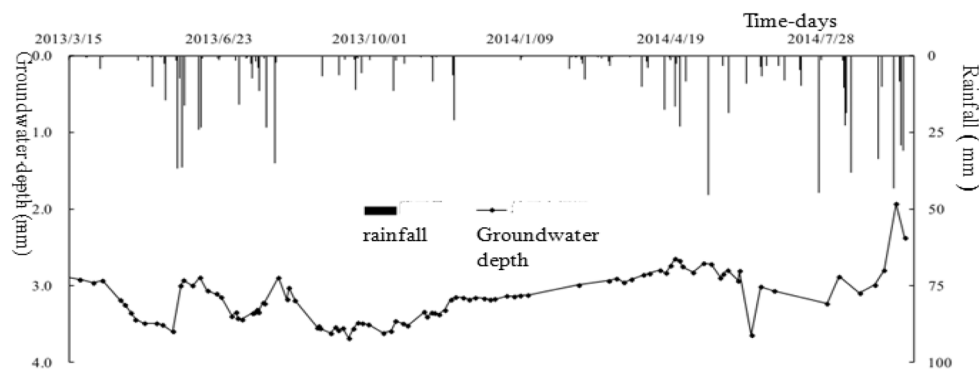
b Data of 2013–2014 (Tang 2016)

Fig. 7 Time variations of groundwater depth. **a** Data of 2016. **b** Data in 2013–2014

Influence of rainfall infiltration on groundwater quality

A total of 165 sets of rainfall quality data were collected during the entire monitoring period (May to October 2016). Fifty-five of the datasets were about influent water quality data, groundwater quality data before rainfall, and groundwater quality data after rainfall. The maximum concentrations of water in #2 and #3 from May to October are shown in Table 3 and Fig. 8. The groundwater concentrations of COD, NH_4^+-N, and TP in the rain gardens were less than those in the surface water. The adsorption of soil and other fillers reduced the concentration of pollutants by 50–90%. The main reason is that the groundwater is located in the soil water zone below the aeration zone. On the one hand, large amounts of enzymes and microorganisms exist in the soil zone in the aeration zone; they play an important role in the degradation of N and P in groundwater and therefore can be converted into

Table 3 Influence of water quality concentration on the rain gardens

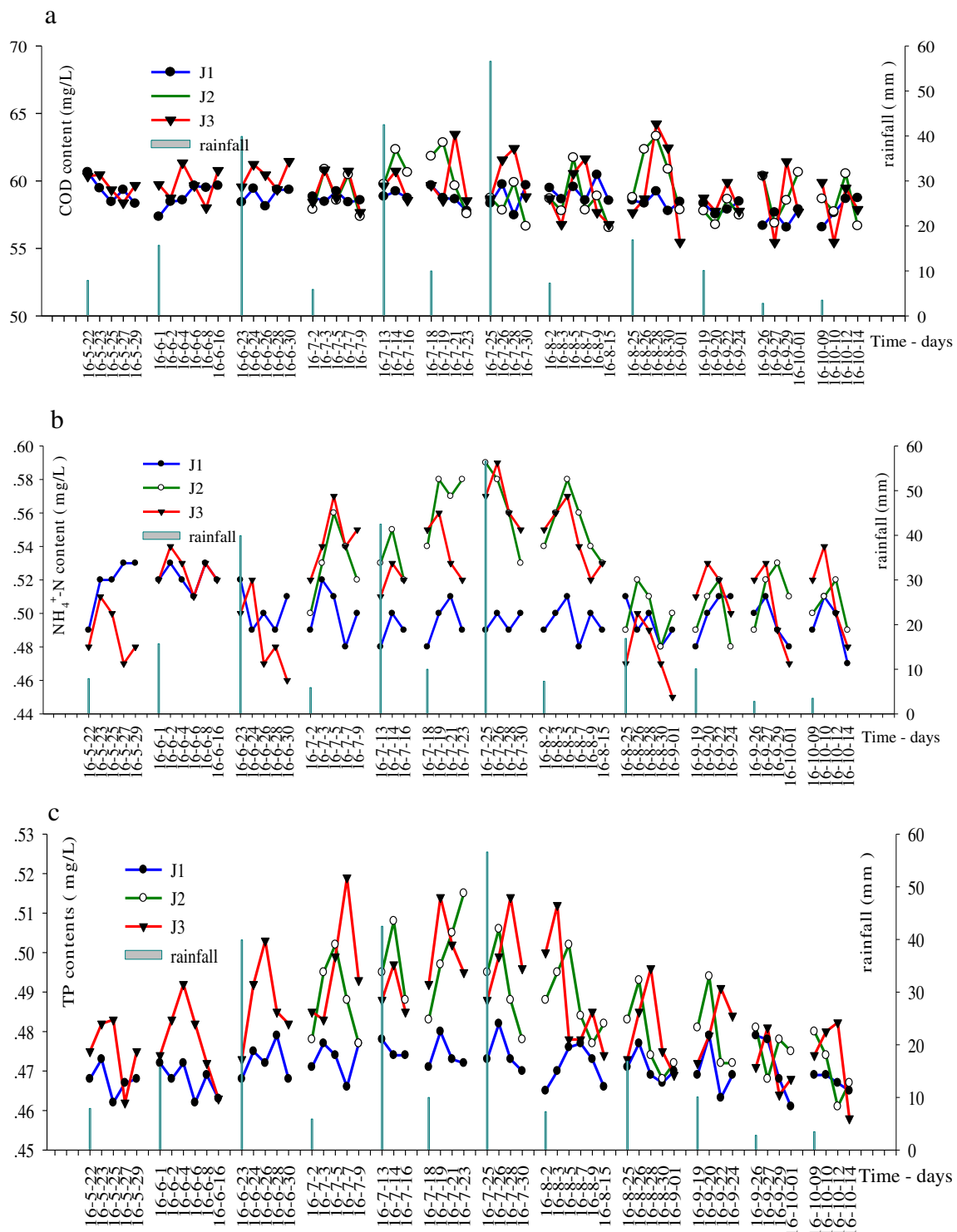| Months	#2 water quality					#3 water quality				
	COD (mg/L)	NH_4^+-N (mg/L)	NO_3^--N (mg/L)	TN (mg/L)	TP (mg/L)	COD (mg/L)	NH_4^+-N (mg/L)	NO_3^--N (mg/L)	TN (mg/L)	TP (mg/L)
5	128.56	2.43	1.49	4.02	0.755	136.37	2.25	1.35	3.86	0.747
6	150.53	2.36	1.665	4.055	0.872	139.27	2.4	1.405	3.7	1.253
7	135.615	2.115	1.4975	3.93	1	122.368	2.238	1.305	3.84	0.879
8	151.875	2.545	1.59	4.335	0.957	140.89	2.335	1.38	4.065	1.023
9	111.03	2.115	1.3	3.36	0.785	128.33	2.105	1.205	3.18	0.783
10	128.73	2.34	1.35	3.78	0.845	118.81	2.12	1.37	3.45	0.817

Fig. 8 Change process of groundwater quality in groundwater before and after rainfall. **a** Change process of COD content in underground water. **b** Change process of NH$_4^+$-N content in underground water. **c** Change process of TP content in underground water

an ionic form for plant growth. On the other hand, the groundwater in the water pack has a certain self-purification capability, which can further degrade COD, N, and P in the groundwater; thus, its content was reduced (Guo et al. 2017). The concentrations of COD, NH$_4^+$-N, and TP of groundwater in

the monitoring wells were listed within the monitoring period and within 3 days after rainfall (Tables 4 and 5). The t test of COD observations was insignificant, which indicated that concentrated infiltration of rainwater gardens would not affect COD concentration in groundwater. The t test results of NH$_4^+$-

Table 4 Statistical results for COD, NH_4^+-N, and TP concentrations in groundwater

Well number	COD			NH_4^+-N			TP		
	Avg ± SD	Max	Min	Avg ± SD	Max	Min	Avg ± SD	Max	Min
J1	58.6311 ± 0.873	60.65	56.56	0.2873 ± 0.013	0.31	0.26	0.4711 ± 0.005	0.482	0.461
J2	59.1841 ± 1.882	63.32	56.54	0.3164 ± 0.023	0.38	0.27	0.4851 ± 0.128	0.515	0.461
J3	59.4162 ± 1.858	64.23	55.45	0.3144 ± 0.25	0.37	0.26	0.4847 ± 0.136	0.51	0.458

N and TP observations in J2 were significant, which implied that the infiltration volume of rainwater gardens significantly increased the concentration of NH_4^+-N and TP in groundwater. Table 3 shows that the difference in influent concentration between #2 and #3 is insignificant. The groundwater concentration of J2 was significantly different from that of J1, which indicated that the purification effects of NH_4^+-N and TP in the loess area were worse than those in layered packing. The concentrations of COD, NH_4^+-N, and TP in J1, J2, and J3 first increased with the rainfall and then decreased. The concentration changes exhibited the same trend during the entire monitoring process. The groundwater quality concentrations of J2 and J3 were greater than that of J1 when the rainfall was relatively large during July–August 2016. The accumulation of rainfall hence exerted a certain impact on groundwater quality. Concentrated infiltration of rainwater gardens will increase the concentration of groundwater and will be affected by the cumulative amount of rainfall.

Analysis of concentrated infiltration of water recharge and infiltration coefficient

Most of surface water are trapped by plants, retained in pits, and eventually consumed in evaporation. Only a small amount of infiltration water is supplied to the groundwater. When the rainfall intensity is less than the infiltration rate, the surface water will infiltrate into the aquifer in large quantities. When

the rain is stronger than the infiltration rate, the surface water may overflow the garden pit and increase the pressure of the urban drainage network. Rainfall time, recharge, water level change, and recharge coefficient of groundwater were needed, as shown in Table 6, to accurately study the recharge of groundwater by rainfall. The data showed a large difference in recharge in case of different rainfall. When the confluence flow was the same, the recharge of #2 garden was greater than that of #3 garden, which indicated that the recharge of loess area is greater than that of layered filling area. Zhu et al. (2010) found that the recharge of the loess area is the largest, followed by that in the riverhead area, and the smallest is in the windy sand area in the study of changes of groundwater recharge and discharge in the watershed of the Loess Plateau. Therefore, the loess area could better protect groundwater resources and utilize rainwater resources.

Model setup and discussion

Groundwater numerical simulation commonly uses analytical methods, which include finite difference and finite element methods. The finite difference method is based on the basic differential equation of groundwater flow and definite condition. The solution of the differential equation of groundwater flow is transformed into a difference equation by using a difference operator instead of a derivative based on the

Table 5 Statistical results for pollutant concentration in groundwater-monitoring wells

Pollutant	Well number	Monitoring period			Within 3 days		
		Avg ± SD	t	p	Avg ± SD	t	p
COD	J1	58.6311 ± 0.873			58.5058 ± 0.920		
	J2	59.1841 ± 1.882	0.146	0.376[☆]	59.6070 ± 1.870	0.347	0.076[☆]
	J3	59.4162 ± 1.858	0.066	0.631[☆]	59.6522 ± 1.864	0.158	0.357[☆]
NH_4^+-N	J1	0.2873 ± 0.013			0.2878 ± 0.014		
	J2	0.3164 ± 0.023	0.515	0.001*	0.3222 ± 0.024	0.521	0.005*
	J3	0.3144 ± 0.25	0.171	0.211[☆]	0.3186 ± 0.026	0.117	0.498[☆]
TP	J1	0.4711 ± 0.005			0.4718 ± 0.004		
	J2	0.4851 ± 0.128	0.51	0.001*	0.4876 ± 0.122	0.544	0.003*
	J3	0.4847 ± 0.136	0.295	0.029[☆]	0.4857 ± 0.013	0.271	0.095[☆]

*$p < 0.01$, the difference is significant

[☆] $p > 0.01$, the difference is insignificant

Table 6 Rainfall time, interception by vegetation, height difference of groundwater depth, groundwater recharge, recharge coefficient, and evaporation coefficient of precipitation

|	Month Unit	Time day	P mm	Q mm	$\triangle H$ mm	P_r mm	E mm	a	Recharge mm/year
#2	July	2016-07-02	5.9	112.1	150	31.2	68.42	0.278	1173.12
		2016-07-13	42.5	807.5	130	27.04	780.46	0.033	
		2016-07-18	10	190	110	22.88	158.8	0.120	
		2016-07-25	56.6	1075.4	80	16.64	1040.04	0.015	
	August	2016-08-02	7.3	138.7	80	16.64	84.62	0.120	274.56
		2016-08-25	16.9	321.1	30	6.24	300.3	0.019	
	September	2016-09-19	10.1	191.9	140	29.12	152.38	0.151	424.32
		2016-09-26	2.8	53.2	30	6.24	36.56	0.117	
	October	2016-10-09	3.5	66.5	50	10.4	49.86	0.156	124.8
#3	May	2016-05-22	7.9	114.55	20	4.16	106.23	0.036	49.92
	June	2016-06-01	15.7	227.65	50	10.4	194.37	0.046	374.4
		2016-06-23	39.9	578.55	100	20.8	545.27	0.036	
	July	2016-07-02	5.9	85.55	50	10.4	66.83	0.122	574.08
		2016-07-13	42.5	616.25	40	8.32	607.93	0.014	
		2016-07-18	10	145	80	16.64	117.96	0.115	
		2016-07-25	56.6	820.7	60	12.48	806.14	0.015	
	August	2016-08-02	7.3	105.85	60	12.48	68.41	0.118	449.28
		2016-08-25	16.9	245.05	120	24.96	209.69	0.102	
	September	2016-09-19	10.1	146.45	30	6.24	138.13	0.043	74.88
		2016-09-26	2.8	40.6	0	0	34.36	0	
	October	2016-10-09	3.5	50.75	30	6.24	38.27	0.123	6.24

Q the interception by vegetation (mm)

subdivision of the seepage zone. The finite element method divides the computational domain into a finite number of non-overlapping units. The problem of describing the solution of groundwater flow is transformed into a definite equation by the method of division and interpolation to be dispersed in each unit (Jin and Qin 2016). The finite difference method is more frequently used than the finite element method in the treatment of an aquifer boundary; its calculation and solution method are also simpler. The finite difference method has high accuracy in solving the groundwater flow problem.

Model establishment of study area

Mathematical discretization of the nodes in the geological part of the simulated area should be performed to transform the complicated seepage problem of groundwater into simple and regular seepage problems in the cross-section cells after the establishment of the mathematical model of groundwater flow and groundwater quality in the study area. The finite difference method was used in this numerical simulation to study the influence of centralized infiltration of rain gardens on the groundwater level. The study area was regarded as a 3D isotropic homogenous medium after analysis of the groundwater levels of J1, J2, and J3 for 180 days. The distance of the mathematical model grid subdivision significantly affects the accuracy of the mathematical model operation and the efficiency of program operation when the computer hardware and programming data structure are fixed. The study area covers two rain gardens, as shown in Fig. 9.

Fig. 9 Meteorological condition and precipitation infiltration recharge of the study area
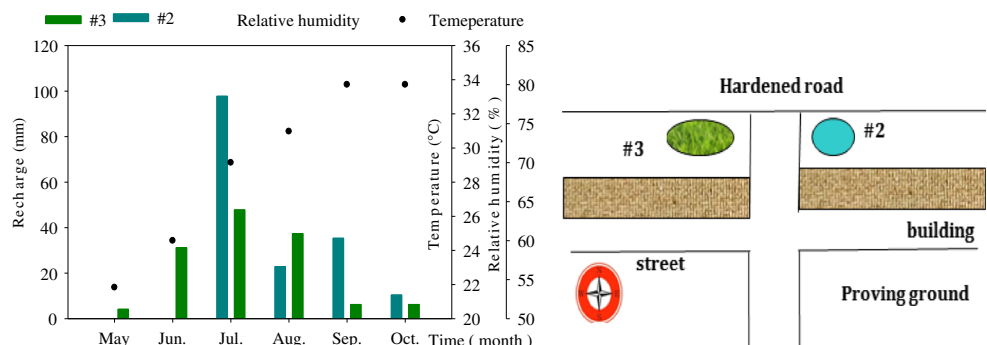
Parameter partitioning

Visual MODFLOW can reduce the complexity of mathematical modeling. The operation is simple, the processing of data and maps is efficient, the simulation results can be visualized, and the output greatly improves work efficiency. The parameters of the simulation area partitioning objectively reflect the basic premise of the hydrogeological conditions and the model parameters, including external (source, boundary condition, evaporation, etc.) and internal (seepage velocity, storage coefficient, specific yield, and porosity, etc.) parameters.

Hydraulic conductivity of the study area by the average annual dynamic data groundwater observation and experiment was 2.7×10^{-5} m. The study area is small, and the groundwater medium is relatively uniform. Thus, the hydraulic coefficient of the entire study area had the same value as that in a traditional practice. The #2 medium is the local loess, and #3 is the layered filler. The garden soil samples were determined to be silt–sand, and the silt–sand content slowly increased over time and reached 73.49% by the end of 2015. The water storage coefficient is 10^{-5} m^{-1}, the gravity-specific yield is

0.208, the effective porosity is 0.3, and the total porosity is 0.3. Research on groundwater recharge was mainly based on atmospheric precipitation in the study area. Gardens #2 and #3 belong to large depressions. The relationship of rainfall supply, relative humidity, and temperature, as well as different rain garden supplies according to the rainfall infiltration model, are both shown in Fig. 9. The selection of initial groundwater level was derived from the actual monitoring data of observation wells apart from the experimental rain garden. The results of several observations from 2016 to 2017 showed that the groundwater level rebounded after the rainy season and that the groundwater depth in the winter slightly decreased. The initial groundwater depth of 4 m was studied according to the monitoring data analysis. The length of the grid X, Y is (50, 40), and the length of each grid is 1 m.

Modeling results

The mathematical model was calibrated by the groundwater level dynamic observation data during the period of water from May 22, 2016, to August 2, 2016, to verify the reliability of
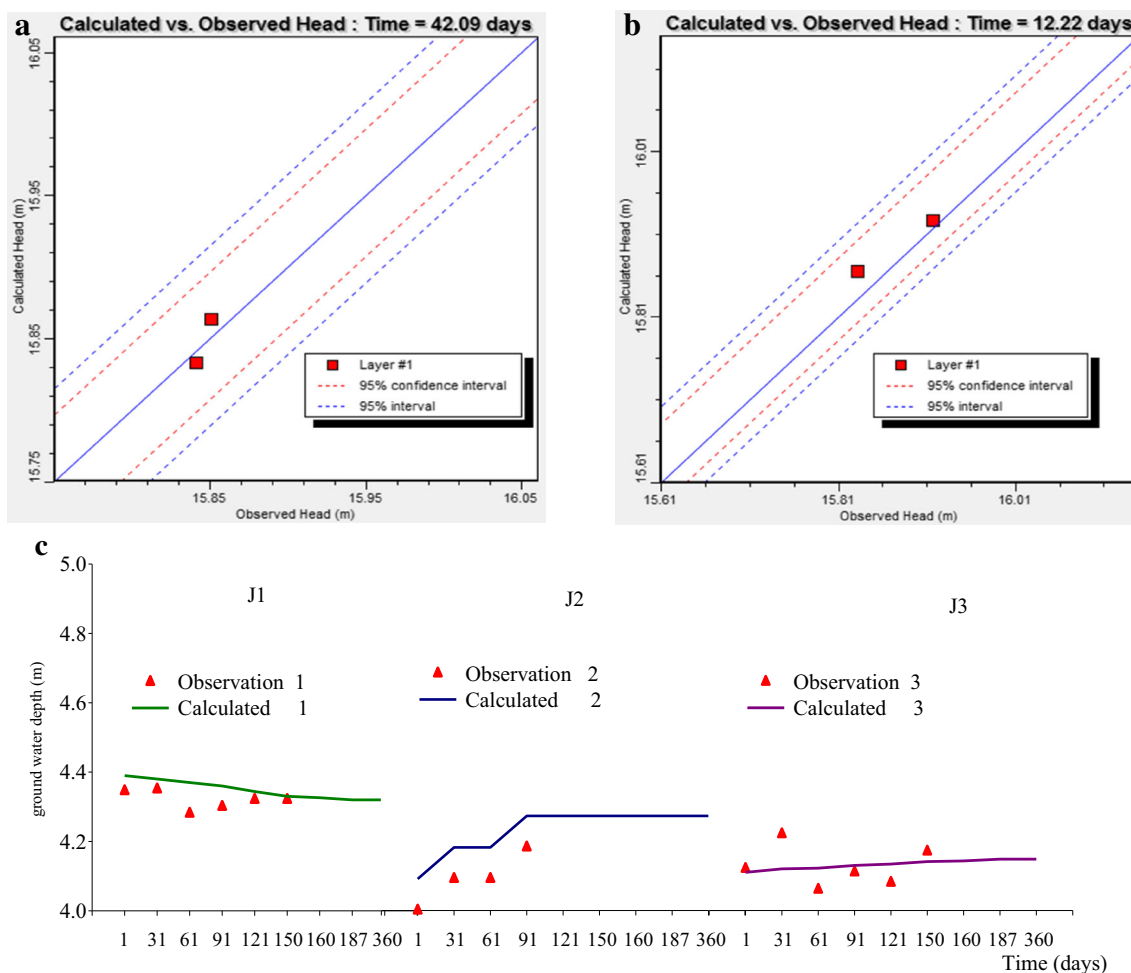

Fig. 10 Comparison of the results between measured and simulated data in model calibration (**a**). Comparison of the results between measured and simulated data in model validation (**b**) and groundwater level fitting (**c**)

Table 7 Various parameters and influencing factors (Zhai et al. 2010)

	Parameter	Influencing factor
External factors	Precipitation infiltration rate	(1) duration of precipitation; (2) rainfall intensity; (3) groundwater level
	Evaporative discharge of phreatic water	(1) evaporation intensity of water surface; (2) underlying surface; (3) underground water level
Internal factors	Hydraulic conductivity	(1) physical properties of percolation liquid; (2) lithology of aquifers; (3) separation of aquifer particles; (4) scale
	Specific yield, storage rate	(1) lithology; (2) bottom structure; (3) groundwater level; (4) scale
	Porosity	(1) lithology; (2) scale

the established mathematical model and model parameters. The mathematical model was validated by using the data of August 25, 2016, to October 9, 2016. The maximum absolute error of groundwater depth is 0.38 m by comparing the simulated and the measured level. The water level fitting results are shown in Fig. 10. The fitting result was acceptable. Thus, the mathematical model developed is in good agreement with the actual situation in the study area, and the generalization of the hydrogeological conditions, the determination of the boundary conditions, and the parameters are completed. The model can accurately predict the depth of water infiltration in the rain gardens.

Parameter sensitivity analysis

Sensitivity analysis of parameters is the measurement index of the calculation results of the numerical model of groundwater flow to change the response degree of these parameters. This measurement index is necessary in groundwater flow and solute transport simulation. Sensitivity is usually indicated by the sensitivity coefficient. When the sensitivity coefficient is high, the influence of the change in the parameter on the calculation result is large. The objectives of sensitivity analysis are to quantify the uncertainties of the identified models and determine the degree of influence of the uncertainty of aquifer, boundary conditions, and external influences on the calculation results of the model for judging the correctness of the model. Uncertainty analysis methods can be divided into the Monte Carlo method, the moment equation method, the Bayesian method, and other methods (such as conditional simulation, sensitivity analysis, and second-order moment method) according to their principle. This study adopted the

sensitivity analysis method based on Morris screening, which is a widely used uncertainty analysis method (Morris, 1991; Sharifan et al. 2010).

Parameters can be divided into external and internal, which include groundwater movement in the process of simulation and migration of water quality simulation parameters. Zheng suggested that the parameter value is in the range of 1–5%, and Wang suggested that parameters, such as the coefficient of permeability of aquifer water level and floating rate, reach 50% (Zhai et al. 2010). The underground water table is not as evident as a seasonal variation. The atmospheric precipitation forms surface water because the depth of the groundwater table is low during the rainfall, which reduces the infiltration volume and increases the buried depth. Most of the infiltration water is filled in the unsaturated soil, thereby gradually decreasing the recharge volume. Hence, groundwater can obtain an ideal maximum infiltration supply at a reasonable burial depth. Various parameters are controlled by various factors, as shown in Table 7. Because the scope of this study area is small, no resupply of rivers and other sources was observed. The influencing factors were determined. The internal factors were analyzed based on the revised Morris screening method and related studies. The internal factors were disturbed by 5% fixed steps, and the disturbances were −20%, −15%, −10%, −5%, +5%, +10%, +15%, and +20% while ensuring that the other parameters are constant. The parametric analysis results are shown in Table 8. The external factors exert greater influences than those of the internal factors, and supply strength is a slightly sensitive parameter. The hydraulic conductivity, storage rate, specific yield, and porosity are insensitive parameters within a small range.

Table 8 Sensitivity analysis results of the hydrodynamic influence

Classification	Parameter	Physical Meaning	Unit	Value Range	Sensitivity Value	Sensitivity Level
External factors	Supply intensity	Rain intensity, rainfall duration	mm/year	38.4–1353.6	$3.81047e^{-5}$	Sensitive
Internal Factors	Penetration Coefficient	Void media, particle characteristics	m^3/day	0.0000216–0.0000324	0	Insensitive
	Water storage rate	Groundwater depth, scale	m/1	0.000008–0.000012	0	Insensitive
	Specific yield	Lithology, scale	–	0.16–0.24	0	Insensitive
	Porosity	Lithology, scale	–	0.24–0.36	0	Insensitive

Conclusions

The water level monitoring in 2013, 2014, and 2016 showed that the groundwater depth of the two rain gardens was stable at 3.0–4.5 m. The water level of J2 and J3 slightly increased after each rainfall event and then decreased. The variation order of the water level of the three wells was J2 > J3 > J1. Rain garden infiltration decreased the depth of the groundwater level, but the supply effect lagged behind. The overall lag was 2 to 3 days. The contents of COD, TN, and TP in J2 and J3 increased after each rainfall event and then decreased gradually. The variation range of COD was approximately 58.6311 ± 0.873 mg/L for control well J1, 59.5841 ± 1.882 mg/L for J2, and 51.4162 ± 1.858 mg/L for J3, the variation range of NH_4^+-N was approximately 0.2873 ± 0.013 mg/L for control well J1, 0.3164 ± 0.023 mg/L for J2, and 0.3144 ± 0.25 mg/L for J3, and the variation range of TP was approximately 0.4711 ± 0.005 mg/L for control well J1, 0.4851 ± 0.128 mg/L for J2, and 0.4847 ± 0.136 mg/L for J3. This result indicated that the centralized infiltration of rainwater gardens will not affect the safety of groundwater at a certain scale, and it is conducive to the conservation of groundwater sources.

A geological conceptual model of the groundwater simulation system was established with the Visual MODFLOW software, which is generalized as the isotropic homogeneous 3D unsteady flow mathematical model. The actual geologic conceptual model of rain gardens was objectively reflected by confirming the hydrogeological parameters. Therefore, the established model is close to the actual groundwater system. The results of the simulation objectively reflected the change in groundwater depth of the rain gardens according to the model calibration and validation.

References

Arnold JG, Muttiah RS, Srinivasan R, Allen PM (2000) Regional estimation of base flow and groundwater recharge in the Upper Mississippi River basin. J Hydrol 227:21–40

Crosbie R S, Binning P, Kalma J D (2005) A time series approach to inferring groundwater recharge using the water table fluctuation method. Water Resour Res 41:1-8

Forrer R, Kasteel M, Flury H (1999) Flühler longitudinal and lateral dispersion in an unsaturated field soil. Water Resou Res 35:3049–3060

Fan Y, Zhao ZG, Huang X, Jia LJ, Lu HY (2015) Numerical simulation of groundwater in Tenglong terrace based on Visual MODFLOW. J Water Resour Archit Eng 13:195–200 **in Chinese**

Gerla PJ (1992) The relationship of water-table changes to the capillary fringe, evapotranspiration, and precipitation in intermittent wetlands. Wetlands 12:91–98

Guo C, Li JK, Li HE, Ma MH, Zhang B, Zhao RS (2017) Rainwater garden concentration infiltration on the groundwater level and water quality. J Hydroelectr Eng 36:49–60 **in Chinese**

Jia ZH, Wu SR, Tang SC, Luo Z, Xu Q, Shao ZX, Ma XY (2018) Influences of focused recharge from rain gardens on groundwater level and water quality. Adv Water Sci 29:221–229

Jin YL, Qin JA (2016) Research on numerical simulation of contaminant transportion in groundwater and its application review. Ground Water 38:21–23 **in Chinese**

Lu YT, Tang CY, Chen JY, Chen JH (2015) Groundwater Recharge and Hydrogeochemical Evolution in Leizhou Peninsula, China. J Chem 2015:1-12

Li JQ, Xiang LL, Mao K, Li BH, Li HY, Che W (2010) Case analysis of rainwater garden soil infiltration disposal roof runoff. China Water Wastewater 26:129–133 **in Chinese**

Loheide SP, Butler JJ, Gorelick SM (2005) Estimation of groundwater consumption by phreatophytes using diurnal water table fluctuations: a saturated-unsaturated flow assessment. Water Resour Res 41:372–380

MACHUSICK M, WELLKER A, TRAVER R (2011) Groundwater mounding at a storm-water infiltration BMP. J Irrig Drain E-asce 137:154–160

Morris MD (1991) Factorial sampling plans for preliminary computational experiments. Technometrics 33:161–174

Phillips IR (2006) Modelling water and chemical transport in large undisturbed soil cores using HYDRUS-2D. Soil Res 44:27–34

Rantz SE (1982) Measurement and computation of streamflow: volume 1. Measurement of stage and discharge. Geol Surv Water-Supply Pap 1:211-226

Raj MS, Prabhakar S (2016) Groundwater system simulation and management using Visual MODFLOW and Arc-SWAT. International Conference 5:29–35

Schilling KE, Kiniry JR (2007) Estimation of evapotranspiration by reed canary grass using field observations and model simulations. J Hydrol 337:356–363

Scholz M, Grabowiecki P (2007) Review of permeable pavement systems. Build Environ 42:3830–3836

Sharifan RA, Roshan A, Aflatoni M, Jahedi A, Zolghadr M (2010) Uncertainty and sensitivity analysis of SWMM model in computation of manhole water depth and subcatchment peak flood. Procedia Soc Behav Sci 2:7739–7740

Tang SC (2016) Study on regulation of rain - fed and flood runoff by small and medium green infrastructure in Sponge City. Dissertation. Xi'an University of Technology., Xi'an China. (in Chinese)

Ting CS, Kerh T, Liao CJ (1998) Estimation of groundwater recharge using the chloride mass-balance method, Pingtung Plain, Taiwan. Hydrogeol J 6:282–292

Van RM (2007) Water localisation and reclamation: steps towards low impact urban design and development. J Environ Manag 83:437

Watson A, Miller J, Fleischer M, Clercq WD (2018) Estimation of groundwater recharge via percolation outputs from a rainfall/runoff model for the Verlorenvlei estuarine system, west coast, South Africa. J Hydrol 558:238–254

Wu DJ, Zhan SZ, Li YH, Tu MZ, Zu JY, Guo YY (2016) New trend and practice of Sponge City with Chinese characteristics. China Soft Science 1:79–97 **(in Chinese)**

Yang H, Dick WA, Mccoy EL, Phelan PL, Grewal PS (2013) Field evaluation of a new biphasic rain garden for storm water flow management and pollutant removal. Eco Eng 54:22–31

Yu KJ, Li DH, Yuan H, Fu W, Qiao Q, Wang SS (2015) Theory and practice of "Sponge City". City planning 39:26–36 **in Chinese**

Zhu RR, Zheng HX, Liu CM (2010) Changes of groundwater recharge and discharge in water shed of the Loess Plateau. Sci Geogr sci 30: 108–112.**(in Chinese)**

Zhai YZ, Wang JS, Su XS (2010) Parameter sensitivity analysis in groundwater numerical simulation. People's Yellow River 32:99–101 **(in Chinese)**

Zimmer CA, Heathcote IW, Whiteley HR, Schroter H (2007) Low impact development practices for storm water: implications for urban hydrology. Can Water Resour J 32:193–212

Publisher's note Springer Nature remains neutral with regard to jurisdictional claims in published maps and institutional affiliations.